Influence of Strain on the Conduction Band Structure of Strained Silicon Nanomembranes

C. Euaruksakul, Z. W. Li, F. Zheng, F. J. Himpsel, C. S. Ritz, B. Tanto, D. E. Savage, X. S. Liu, and M. G. Lagally
University of Wisconsin-Madison, Madison, Wisconsin 53706, USA
(Received 16 February 2008; published 3 October 2008)

The influence of in-plane biaxial strain on the conduction bands of Si is explored using elastically strained Si(001) nanomembranes and high-resolution x-ray absorption measurements with electron yield detection. The strain-induced splitting of the conduction band minimum and the energy shifts of two higher conduction bands near L_1 and L_3 are clearly resolved. The linear increase of the splitting of the conduction band minimum with increasing strain and the nonlinear shift of the L_1 point toward the conduction band minimum agree quantitatively with current theories.

DOI: 10.1103/PhysRevLett.101.147403 PACS numbers: 78.40.Fy, 71.20.Mq, 71.70.Fk

There is currently enormous interest in employing very thin Si films with high strain. Strained Si (sSi) significantly increases the mobility of charge carriers [1]. In field effect transistor devices, thin Si used as the channel reduces short-channel effects (the expansion of source and drain regions to shorten the effective length of the channel) [2]. Advanced complementary metal-oxide-semiconductor imaging systems will gain in resolution and speed by using strained Si. Very fast flexible electronics needed in macro-electronics, radio frequency identification, electronic-paper, and similar technologies require transferred thin single-crystal Si [3], with relevant properties significantly enhanced by using strained Si [4]. In all electronic-device applications that require both speed and mechanical flexibility, thin strained Si membranes or films will provide distinct advantages.

The sensitive dependence of carrier mobility on strain, combined with the thinness and flexibility of Si required in these advanced applications, makes the quantitative measurement of strain, its distribution, and its effect on the band structure of extremely thin Si layers highly desirable, especially in elastically strain sharing silicon nanomembranes (SiNMs), a relatively new nanomaterial [5,6]. Recent work has demonstrated that it is possible to obtain high levels of tensile strain in Si—without the dislocations or surface roughness that are inherent in conventionally prepared strained Si or SiGe alloy [7]—via the fabrication of Si nanomembranes. These SiNMs are made, for example, by heteroepitaxially growing a pseudomorphic film of (compressively strained) SiGe alloy on a thinned Si top layer of silicon-on-insulator, followed by another Si layer. This layer structure is then released by etching the oxide supporting it, to form a membrane that is freestanding in at least part of its fabrication cycle. During the time the SiNM is free of constraints, the compressive strain in the SiGe alloy layer becomes elastically shared with the Si layers, forming very thin tensilely (biaxial, in the plane) strained Si sandwiching compressively strained SiGe alloy. The SiNM can then be transferred to a new host [5].

Figure 1(a) shows schematically aspects of the band structure of Si and the influence of strain on conduction bands. Lattice strain alters the valence and conduction bands by shifting them in energy, distorting them, and removing degeneracy [8]. For Si(001), the 6 degenerate conduction band minima along the ⟨100⟩ axes split into two groups when applying biaxial strain [Δ_4 and Δ_2 in Fig. 1(a)]. For tensile strain, the energy of the two Δ_2 valleys [perpendicular to the (001) plane] is lowered (caused by a uniaxial strain component out of the plane resulting from the in-plane biaxial tension), while that of the four equivalent in-plane Δ_4 valleys is raised, relative to their center of gravity, which may also shift in energy. Compressive strain causes similar behaviors, with the directions of splitting of Δ_4 and Δ_2 reversing [9,10]. Other components of the conduction band structure are also affected by strain.

The novelty of the work presented here lies in our ability to make very thin sheets of elastically strained Si that are perfect crystals in which we know the strain [5], and to measure the positions of electronic bands quantitatively in these sheets. In very thin strained-Si layers, determining the relationship between strain and band structure is a challenge. We use high-resolution soft-x-ray absorption spectroscopy (XAS) to establish the influence of strain on several critical points in the conduction band. Electron yield detection makes it possible to do so in very thin films, because of the shallow probing depth of low-energy electrons (a few nm) [11]. The measured electron current consists primarily of secondary electrons that originate from Auger electrons. Monochromatized photons (with 10 meV resolution) from the University of Wisconsin Synchrotron Radiation Center are used to excite transitions from the $2p$ core level of Si into the conduction band [the $L_{\mathrm{II,III}}$ lines, ~100 eV]. The Lorentzian linewidth of the $2p$ level is ~45 meV [12]. The spatial resolution is ~1 mm but our membranes are uniform over much larger areas.

To explore the effect of strain on the conduction band structure of Si, we use strained SiNMs with four tensile-strain conditions, 0.325%, 0.630%, 0.800%, and 0.950%. The 0.325% and 0.630% strained Si samples are created by releasing 23 nm Si/107 nm $Si_{0.87}Ge_{0.13}$/28 nm Si and 4 nm Si/69 nm $Si_{0.8}Ge_{0.2}$/9 nm Si sandwich structures,

 © 2008 The American Physical Society

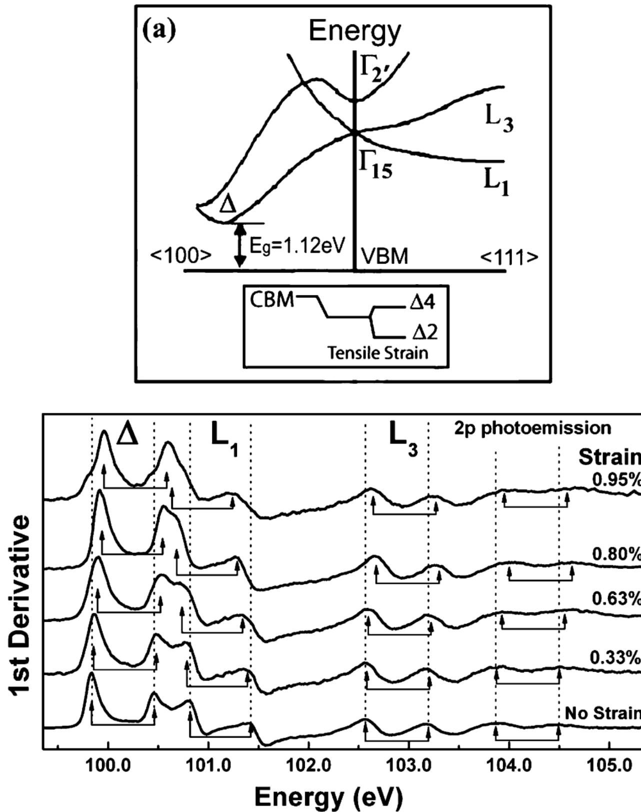

FIG. 1. Effect of strain on the conduction bands of Si: (a) Illustration of the band structure of unstrained Si showing the global minimum along Δ and local extrema at L_1 and L_3, after [6]. The inset shows how in-plane tensile strain modifies the conduction band minimum (CBM). (b) Derivative x-ray absorption spectra. The $2p \rightarrow \Delta$ and $2p \rightarrow L_3$ transitions increase in energy while the $2p \rightarrow L_1$ transition decreases. The arrows for Δ mark the center of gravity of the split Δ_2, Δ_4 bands. All features are duplicated because of the spin-orbit splitting of the $2p$ core level into $2p_{3/2}$ and $2p_{1/2}$. All spectra are normalized with x-ray intensity and offset so they do not overlap each other.

respectively. The 0.800% strained Si sample is traditionally fabricated [13] by an epitaxial growth of a pseudomorphic 20 nm Si film on a fully relaxed SiGe buffer layer grown on a Si substrate by chemical vapor deposition. The 0.950% strained Si, the highest strain in this study, is fabricated in the same way as the 0.325% and 0.630% strained Si except that the initial substrate is SiGe-on-insulator with fully relaxed $Si_{0.8}Ge_{0.2}$ as a template layer instead of Si. A high-Ge-concentration SiGe film can be epitaxially grown on this substrate to a much greater thickness than the critical thickness of the same SiGe film grown on bulk Si, without creating new dislocations or severe roughness in the film. The ability to grow high-Ge-concentration SiGe layers results in a larger strain in the subsequent Si layer grown on top, after the structure (13 nm Si/105 nm $Si_{0.7}Ge_{0.3}$/32 nm $Si_{0.8}Ge_{0.2}$) is released. We deduced the strain from x-ray diffraction composition and thickness measurements and checked the strain, where possible (i.e., the thicker membranes), with UV Raman spectroscopy [14]. As a standard we used an unstrained bulk Si substrate. Samples were introduced into UHV immediately after cleaning with hydrofluoric acid and are thus all H-terminated.

To test the reproducibility of the photon energy calibration at the 10^{-4} level, we bracket the measurement of each spectrum of a strained layer by measurements on an unstrained Si reference sample. During the XAS measurement, electron-core hole interactions in the excited state change the shape of the density of states in the conduction band [15]. The change is strong near the conduction-band minimum (CBM) and gradually becomes weaker at higher energy. We can, however, assume that the effect is independent of strain. It is eliminated by considering only strain-induced shifts relative to unstrained Si.

In order to accentuate the strain-induced fine structure we differentiate the x-ray absorption curves [16] with 9-point second-order Savitzky-Golay smoothing. Thereby the step-like onset of the Si $2p$ absorption becomes a well-defined peak, as shown in Fig. 1(b) (lowest peak at 99.85 eV). It corresponds to the transition from the $Si2p_{3/2}$ core level to the CBM (Δ), which provides a convenient reference point [17]. As is obvious in Fig. 1(b), the effect of strain can be observed with XAS not only for the CBM, but also for higher-lying conduction band features that are not accessible by electrical measurements. The two peaks in the energy range 100.8–101.4 eV arise from the transition of $2p_{3/2}$ and $2p_{1/2}$ core-level electrons to the eightfold degenerate L_1 valleys in the conduction band, while at ~103 eV, we can observe absorption peaks due to the transition from $2p$ to the L_3 valley. The shifts with strain shown in Fig. 1(b) will be discussed in more detail later.

We first address the splitting of the conduction band minimum (Δ). Already in Fig. 1(b) one can detect a shoulder on the low-energy side of the Δ peak, which originates from the split-off Δ_2 conduction band minimum. This shoulder is brought out more clearly on an expanded scale in Fig. 2. We are able to reconstruct the spectrum of strained Si by taking the line shape from the spectrum of unstrained Si and duplicating it with the appropriate 2:4 intensity ratio for Δ_2: Δ_4 [11,16,18]. A common energy shift allows for a change in the center of gravity. By using actual Si data for this construction, we are left with only two fit parameters, the Δ_2-Δ_4 splitting of the two components and the shift of their center of gravity. The resulting fit to the strained-SiNM spectrum is shown in Fig. 2(b). The resulting values of the Δ_2 and Δ_4 splitting are plotted versus the tensile strain in Fig. 3. They are close to the theoretical results [10,19–21].

We next address the shifts in absorption energies shown in Fig. 1(b). The change with strain in the optical transition energies from the $2p$ levels to three conduction band features are shown in Fig. 4. The transitions to Δ and L_3

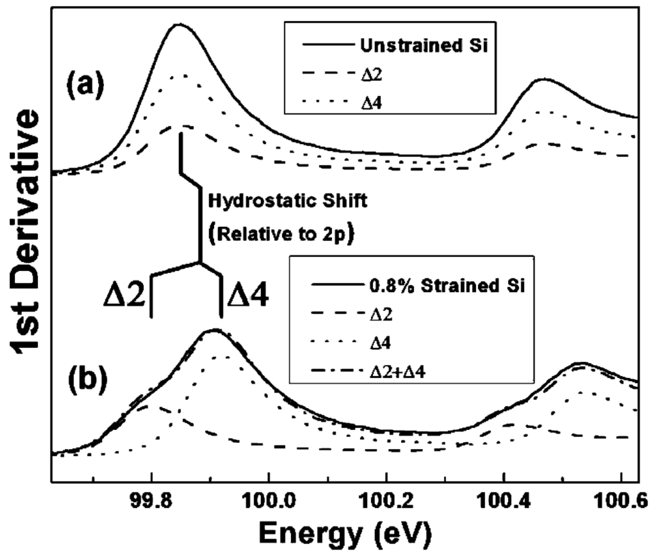

FIG. 2. Derivative of the Si $2p$ absorption edges for (a) unstrained silicon and (b) 0.8% strained Si showing the onset of transitions to the conduction band edge as peaks. The peak corresponding to the conduction band minimum Δ is shifted up in energy and broadened for the strained layer. In (a), the first conduction band peak is decomposed into two components for the Δ_4 (dotted) and Δ_2 (dashed) conduction band minima by scaling down with $2/3$ and $1/3$ multiplicity ratios, respectively. With shift and splitting as fitting parameters, a new peak is reconstructed (dot-dashed line) to match the strained-Si peak in (b).

increase in energy while the transition to L_1 decreases. This opposite shift can directly be seen in Fig. 1(b) where the upper peak merges with the lower L_1 peak at high strain. Such opposite behavior of different conduction band points clearly calls for a more sophisticated explanation than a rigid-band model. By comparing these relative shifts, one concludes that the L_1 point shifts down relative to $\langle\Delta\rangle$ (closer to $\langle\Delta\rangle$), while the higher-lying L_3 point remains at approximately the same energy distance from $\langle\Delta\rangle$. It is evident that relative shifts are of the order of 80–150 meV for a strain of 1%.

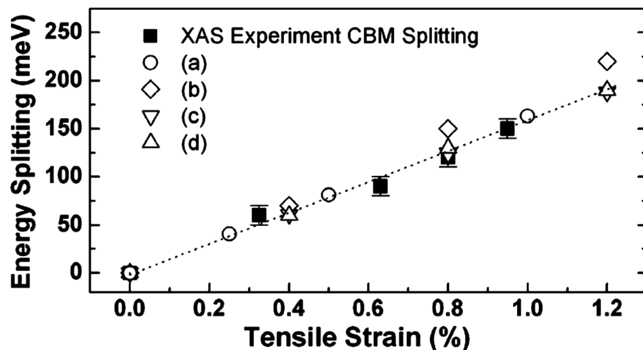

FIG. 3. Splitting of the Si(001) conduction band minimum (Δ) with increasing strain, from fitting experimental results with Δ_2 and Δ_4 components, compared with calculations [(a) Ref. [10], (b) Ref. [19], (c) Ref. [20], (d) Ref. [21]].

Unfortunately the changes in optical transition energies with strain provide only relative changes, and the *direction* of the shift may be misleading, because the $2p$ levels may themselves be affected by strain. Although there is no definitive way out of the experimental quandary, we do have one other measure available. Also observable in the XAS spectrum is the *onset* of photoemission (not a photoemission spectrum). The photon energies for the photoelectric threshold of the Si$2p$ level are seen in the rightmost peaks in Fig. 1(b). A careful analysis [22] of these peaks leads to the determination of the dependence on strain of the onset energies (core level to vacuum level) for Si$2p$ photoemission, shown in the top panel of Fig. 4. A comparison of the top panel with the other three panels of Fig. 4 then suggests qualitatively that all measured conduction band points move to somewhat deeper energies relative to the vacuum level, but by differing amounts. The $\langle\Delta\rangle$ and L_3 points do not shift significantly relative to the vacuum level with increasing strain, as the Si$2p$-to-vacuum transition and the Si$2p$-to-Δ and Si$2p$-to-L_3 transitions shift by approximately the same amount. The L_1 point clearly moves down relative to the vacuum level.

In the above discussion we explicitly assume that the work function does not change with strain (or thickness, as the zero-strain measurement is on bulk Si). With that

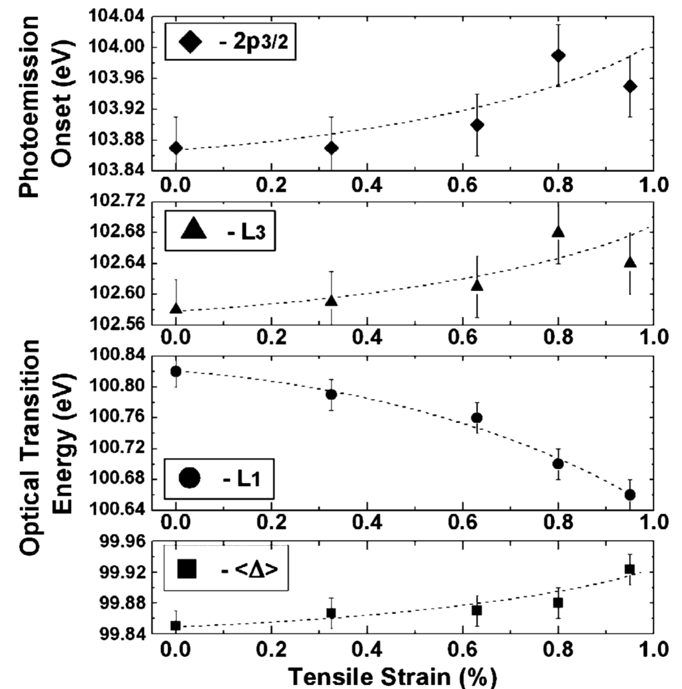

FIG. 4. The change in transition energies of the three conduction band features and the photoemission threshold shown in Fig. 1(b) with increasing tensile strain. The center of gravity has been used for the split Δ_2/Δ_4 band. The L_1 point shifts opposite to L_3 and Δ, demonstrating effects beyond the rigid-band model. The $2p$ photoemission threshold moves to higher energy with increasing strain.

assumption, our results are in agreement with directions of shifts in the absolute-level calculation in [23] but opposite to those in [9,24]. To compare absolute values, it must be remembered that the experiments are on a H-terminated surface.

The reduction of the energy separation of Δ valleys and the L_1 point with increasing tensile strain is consistent with most theoretical calculations [9,19,21,25]. We observe a somewhat greater than linear [9,25] dependence of the $\Delta - L_1$ separation on strain. Degeneracy splitting of the L valleys does not occur with biaxial strain in the plane of Si(001) and we therefore do not expect splitting of the L valleys in Si(001). Dipole selection rules [26] prohibit the transitions from $2p$ level [with Γ_{15} symmetry ($p_{x,y,z}$)] to the Γ_{15} and $\Gamma_{2'}$ critical points.

In summary, via the use of our strain-engineered Si nanomembranes, which are elastically strained, with precisely known and uniform strain, we have quantitatively and reliably determined the dependence of different features of the conduction band on strain, using soft-x-ray absorption spectroscopy with $\sim$10 meV energy resolution. We have demonstrated that we can determine not only the Δ-valley splitting, but also the changes with strain in the optical transition energies of the three lowest conduction bands relative to the $2p$ level. The measurements resolve differences in predictions and quantify magnitudes of strain-dependent band structure modifications. We can also observe the shift in the $2p$ core-level photoemission onset energy. This shift can be used to estimate absolute shifts of conduction band features with increasing strain, with the assumption of a constant work function. Electron energy loss spectroscopy in transmission electron microscopy [27] can in principle also be used for determining conduction band shifts with strain, but it will be difficult to achieve the energy resolution and statistics required to identify the subtle shifts and shape changes that we observe.

A special feature of XAS with electron yield detection is the ability to measure extremely thin films without interference from the support or the host material. As Si nanomembranes become thinner, we expect to see the same strength of XAS signal down to $\sim$2 nm. We can thus project the use of our results in several ways. Because XAS relates strain to the behavior of the conduction band minimum, it relates strain to electron mobilities and to quantum size effects in very thin freestanding membranes or ribbons. We could (1) observe quantum size effects for very thin strained membranes, to make at least qualitative statements about carrier mobility changes with strain at this limit, (2) determine the near-surface strain in thicker films in which the average over depth might not reflect the surface strain, e.g., for bent films, or (3) measure lateral nonuniformities in strain, e.g., in periodically bent membranes [28], by using a focused source of x rays.

Research supported by DOE, Grant No. DE-FG02-03ER46028. The UW-Madison Synchrotron Radiation Center is supported by NSF Grant No. DMR-0537588. The 0.8% strained Si was provided by Dr. Bin Yang, IBM Research Center, Yorktown Heights, NY 10598.

[1] M. L. Lee *et al.*, J. Appl. Phys. **97**, 011101 (2005).
[2] R. H. Dennard *et al.*, IEEE J. Solid-State Circuits **9**, 256 (1974).
[3] R. H. Reuss *et al.*, Proc. IEEE **93**, 1239 (2005).
[4] H. C. Yuan *et al.*, J. Appl. Phys. **100**, 013708 (2006).
[5] M. M. Roberts *et al.*, Nature Mater. **5**, 388 (2006).
[6] S. A. Scott and M. G. Lagally, J. Phys. D **40**, R75 (2007).
[7] J. W. P. Hsu *et al.*, Appl. Phys. Lett. **61**, 1293 (1992).
[8] G. Abstreiter *et al.*, Phys. Rev. Lett. **54**, 2441 (1985).
[9] M. V. Fischetti and S. E. Laux, J. Appl. Phys. **80**, 2234 (1996).
[10] D. Yu and F. Liu, Phys. Rev. B (to be published).
[11] F. J. Himpsel *et al.*, *Photoemission and Absorption Spectroscopy of Solids and Interfaces with Synchrotron Radiation*, edited by M. Campagna and R. Rosei (North Holland, Amsterdam, 1990), p. 203.
[12] J. D. Bozek *et al.*, Phys. Rev. Lett. **65**, 2757 (1990).
[13] F. K. LeGoues, B. S. Meyerson, and J. F. Morar, Phys. Rev. Lett. **66**, 2903 (1991).
[14] J. C. Tsang *et al.*, J. Appl. Phys. **75**, 8098 (1994).
[15] M. Altarelli and D. L. Dexter, Phys. Rev. Lett. **29**, 1100 (1972).
[16] L. J. Huang *et al.*, Phys. Rev. B **50**, 18453 (1994).
[17] The valence band maximum would be another possible reference energy, but we are not measuring valence band states.
[18] F. J. Himpsel *et al.*, Phys. Rev. Lett. **45**, 1112 (1980).
[19] C. G. Van de Walle and R. M. Martin, Phys. Rev. B **34**, 5621 (1986).
[20] S. Richard *et al.*, J. Appl. Phys. **94**, 1795 (2003).
[21] M. M. Rieger and P. Vogl, Phys. Rev. B **48**, 14 276 (1993).
[22] F. Liu, C. Euaruksakul *et al.*, Phys. Rev. (to be published).
[23] C. Tserbak, H. M. Polatoglou, and G. Theodorou, Phys. Rev. B **47**, 7104 (1993).
[24] C. G. Van de Walle, Phys. Rev. B **39**, 1871 (1989).
[25] D. Rideau *et al.*, Phys. Rev. B **74**, 195208 (2006).
[26] W. Eberhardt and F. J. Himpsel, Phys. Rev. B **21**, 5572 (1980).
[27] P. E. Batson, Phys. Rev. Lett. **83**, 4409 (1999).
[28] M. H. Huang *et al.*, Nature Mater. (to be published).